

Joint Spectral Efficiency and Power Allocation Optimization in IEEE 802.16m

Tamer R. Omar and J. Morris Chang, *Senior Member, IEEE*

Abstract—With today's limited bandwidth, high data rate services, and energy efficiency requirements, maximizing the spectral efficiency and minimizing the consumed power becomes essential. Investigating the issues impeding spectral efficiency maximization and consumed power minimization for mobile systems is crucial for solving this contemporary problem. This paper aims to optimize the utilization of the scarce mobile spectrum and the amount of power consumption in the multi-cell IEEE 802.16m networks. A return on investment model adopting a utility optimization technique is proposed; the model objective is to increase the revenue of the mobile service providers by maximizing the normalized spectral efficiency and decrease the operational cost by minimizing the power consumed in the network. Based on this model, we propose two phases scheme (distributed and centralized) to solve the joint spectral and power optimization problem. The problem is solved to identify the optimal distributed resources assignment and the central down-link frequency partition configuration that achieves the model objective. Simulation results show that the optimal solution significantly improves the system power consumption while maintaining the normalized spectral efficiency, yet with high computational complexity. Accordingly, an effective suboptimal solution utilizing a polynomial-time heuristic is proposed for practical implementations.

Index Terms—IEEE 802.16m, normalized spectral efficiency, radio resource management, resource metric

1 INTRODUCTION

THE increased demand for high speed Internet access and mobile Internet services is exponentially driving the development of fourth generation (4G) technologies. 4G networks utilize both the IEEE 802.16 (WiMAX) and the third generation partnership program long term evolution (3GPP-LTE) technologies [1], [2]. Broadband wireless access based on WiMAX standard was approved on October 2010 as an international mobile telecommunication advanced (IMT-Advanced) technology [3]. Optimal radio spectrum utilization and power consumption are crucial in managing WiMAX systems resources.

In WiMAX networks, advanced radio resource management (RRM) schemes that effectively increase spectral efficiency (SE) or decrease power consumption perform a central task in the resource management process. WiMAX introduces a new centralized RRM mechanism called the down-link frequency partition configurations (DFPC) in its latest amendment IEEE 802.16m [4]. This paper aims to determine the optimal DFPC among the list of available DFPCs supported by WiMAX (more details in Section 4) that can efficiently allocate resources in order to achieve the joint maximum normalized spectral efficiency (NSE) and minimum power consumption in the network. The optimal DFPC selection is realized by employing an advanced RRM model.

The RRM model utilizes a centralized semi-static adaptive fractional frequency reuse (AFFR) radio resource allocation scheme. In this research, we aim to select the optimal DFPC through two phases. The first phase adopts a

distributed approach implemented by each advanced base station (ABS) in the network to determine the optimal local DFPC in its cell. The second phase adopts a centralized approach implemented by a higher network control entity (HNCE) which calculates the optimal global DFPC to be utilized in the network using the optimal local DFPCs recommended by each ABS. Fig. 1 shows a flow diagram for the RRM process model. The flow diagram presents the model inputs, processes, decision points, and outputs.

A new two phase (distributed and centralized) scheme is proposed to solve the problem of identifying the optimal DFPC to be utilized in the network. First, the distributed phase problem is formulated as an integer linear program (ILP) which aims at maximizing a newly proposed distributed utility function. The distributed utility function maps the mobile service provider's return on investment (ROI) from utilizing the network. The ROI model proposed aims to increase the mobile service provider's revenues by maximizing the NSE and decrease the cost by minimizing the power consumption. All applicable power and integrality constraints are applied to the formulated problem. Second, the central phase problem is formulated as a utility maximization problem for the average sum of the distributed utility per DFPC achieved by each cell in the network.

The problem solution presented identifies the optimal DFPC that achieves the maximum central utility in the network. A comparison between the performance of the proposed scheme and other rate adaptive resource allocation schemes is conducted (e.g [5], [6]). The results show that the proposed scheme is capable of decreasing the amount of power consumed in the network while maintaining high values for the achievable NSE. The optimal solution demonstrates a high computation complexity. Thus, for practical implementation purposes a suboptimal greedy heuristic algorithm is proposed to reduce the complexity of the optimal solution. The computational complexity analysis for the

• The authors are with the Department of Electrical and Computer Engineering, Iowa State University, Ames, IA 50011.
E-mail: {tomar, morris}@iastate.edu.

Manuscript received 4 May 2014; revised 12 Aug. 2014; accepted 5 Sept. 2014. Date of publication 15 Sept. 2014; date of current version 1 June 2015.
For information on obtaining reprints of this article, please send e-mail to: reprints@ieee.org, and reference the Digital Object Identifier below.
Digital Object Identifier no. 10.1109/TMC.2014.2357809

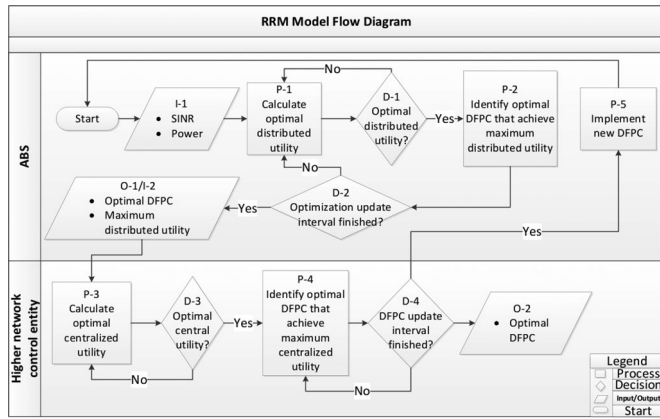


Fig. 1. RRM model flow diagram.

proposed suboptimal greedy algorithm shows that it is a polynomial-time algorithm.

The paper is organized as follows. The related work is discussed in Section 2. The system model is introduced in Section 3. Section 4 provides details about DFPC and the power allocation mechanism. The proposed (centralized and distributed) utilities are presented in Section 5. Central and distributed phase problems formulation are discussed in Section 6. The problem optimal and suboptimal solutions are presented in Section 7. Section 8 presents the simulation and discusses the results. Finally, in Section 9, conclusions are drawn. The acronyms used in this paper are listed and explained in Table 1.

2 RELATED WORK

RRM controls frequency partitioning, multi-connection assignment, and resource units scheduling in the network. Frequency partitions (FPs) in WiMAX divide the cell area into two regions (e.g. cell center and cell edge). Each region utilizes a part of the frequency spectrum. Centralized and distributed static, semi-static, and dynamic fractional frequency reuse (FFR) schemes are proposed in previous research studies to increase the network throughput and SE or to minimize the total power consumption.

The authors in [6] proposed two distributed allocation schemes for FFR operation. First scheme dynamically allocates power across FPs by gradual power adaptation through analysis of the optimal power allocation problem. Second scheme assigns users to achieve load balancing between FPs and performs the assignment with minimum signaling overhead. The results show that the SE can be enhanced by using the proposed schemes under various

network conditions. Using dynamic FFR, the authors in [7] use a utility function for allocating sub-carriers to users according to their geographical regions and then apply opportunistic scheduling for assigning the sub-carriers in each cell. Adaptive modulation and coding techniques are used to increase the throughput and a random access sub-band is applied to improve the fairness of the system.

Graph theory is adopted in [8] and [9] to propose AFFR schemes that improve the cell throughput and the users service rate. The authors in [8] proposed AFFR scheme per cell load conditions to enhance the conventional strict fractional frequency reuse (SFFR). The resource allocation problem is translated into a graph coloring problem where a graph is constructed to match the specific version of the utilized AFFR, followed by coloring the graph using a graph algorithm. A graph-based framework is also proposed in [9] to implement AFFR in a multi-cell network. The scheme utilized enhances the SFFR by enabling adaptive spectral sharing based on cell-load conditions. An interference graph that matches the specific realization of FFR and the network topology is constructed. The graph is colored using a heuristic algorithm. Both proposed schemes offer significant performance improvement in terms of cell throughput and service rate.

Frequency partitioning techniques that aim at mitigating interference are addressed in [10], [11], [12]. Universal frequency reuse (UFR) is presented in [10] to control mutual interference among neighboring cells. The authors assign the whole frequency to all cells and design resource allocation rules to avoid inter-cell interference (ICI). A threshold loading factor is used to maintain ICI at minimum level and increase the spectral reuse efficiency. The results show that the UFR provides high spectral reuse efficiency. AFFR with selected power boosted FPs are discussed in [11] to allow the control of maximum power limits per FP; different power patterns can be employed to determine these limits. In [12] the authors address the joint interaction between interference management and energy utilization. An energy-efficient power optimization scheme is developed for a two-user network with ideal cooperation, then a more generic non-cooperative power optimization scheme is presented to improve the trade-off between energy efficiency and SE. The authors show through simulation in a network with limited interference that the proposed scheme improves the energy and spectral efficiency.

All the previous schemes aimed to maximize either the throughput and SE or minimize the power consumption. Moreover, the scope of all schemes was local using a distributed solution in each ABS. However, the following three

TABLE 1
Table of Acronyms

Acronym	Description	Acronym	Description
ABS	Advanced Base station	FPS	Frequency Partition Size
AMS	Advanced Mobile Station	HNCE	Higher Network Control Entity
DFPC	Down-Link Frequency Partition Configuration	NSE	Normalized Spectral Efficiency
ESE	Expected Spectral Efficiency	PRU	Physical Resource Unit
FFR	Fractional Frequency Reuse	ROI	Return on Investment
FP	Frequency Partition	RRM	Radio Resource Management
FPCT	Frequency Partition Count	SE	Spectral Efficiency

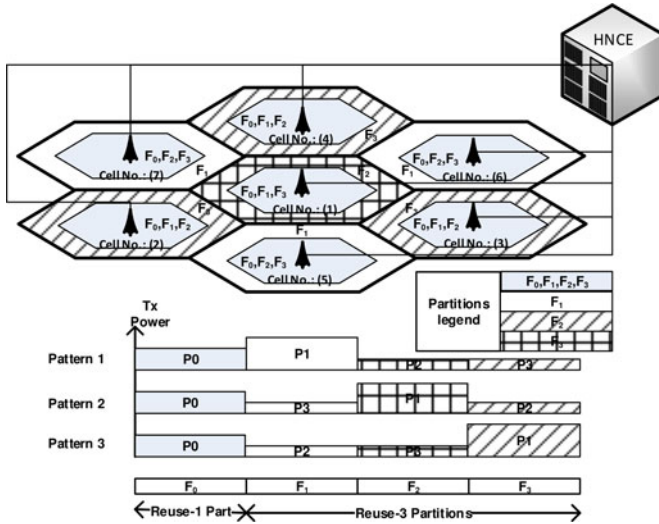


Fig. 2. Network configuration.

important problems that are addressed in this paper were not discussed in previous work:

- 1) Studying the global implementation of the RRM model in the network. For interference mitigation [4] suggests that at any time, one and only one, DFPC can be implemented in the network. This condition results in a conflict between the local optimal DFPC in each cell and the global optimal DFPC in the network which increases the importance of studying the network globally.
- 2) Addressing the DFPCs dynamic behavior according to the network topology, load conditions, and users distribution by identifying the optimal DFPC periodical changes that aims to maximize the utilization of the network resources.
- 3) Using a newly approach in formulating the problem as a joint optimization of the NSE and power consumption to increase the ROI from the network.

3 SYSTEM MODEL

We consider the down-link transmission adopting orthogonal frequency division multiple access (OFDMA) in a multi-cell WiMAX network. The network consists of seven identical adjacent hexagonal cells and a central HNCE responsible for globally controlling the network resources as shown in Fig. 2. It is worse mentioning that the proposed scheme can be applied to other networks that consist of any number of cells. However, the scalability mainly depends on the used topology by the MSPs in implementing their networks.

Each cell contains one centric ABS. The maximum number of cells is B and each cell is denoted by \mathcal{L}_b where $b = \{1, 2, \dots, B\}$. The maximum number of FPs in each cell is M and each FP is denoted by \mathcal{F}_i where $i = \{1, 2, \dots, M\}$. The maximum number of advanced mobile stations (AMSs) with pending traffic in each FP is denoted by S and each AMS is denoted by \mathcal{S}_j where $j = \{1, 2, \dots, S\}$. The number of AMSs differ from one cell FP to another and they are assumed to be uniformly distributed. A physical resource unit (PRU) is the basic physical unit used for resource

TABLE 2
FFT = 2,048, $\mathcal{W} = 20$ MHz

C_c	$\mathcal{F}_0:\mathcal{F}_1:\mathcal{F}_2:\mathcal{F}_3$	FPCT	FPS(PRUs)	$\mathcal{W}_0:\mathcal{W}_1:\mathcal{W}_2:\mathcal{W}_3$
C_1	1:0:0:0	1	96:0:0:0	20:0:0:0
C_2	0:1:1:1	3	0:32:32:32	0:6.67:6.67:6.67
C_3	1:1:1:1	4	24:24:24:24	5:5:5:5
C_4	3:1:1:1		48:16:16:16	10:3.33:3.33:3.33
C_5	5:1:1:1		60:12:12:12	12.5:2.5:2.5:2.5
C_6	9:1:1:1		72:8:8:8	15:1.67:1.67:1.67
C_7	9:5:5:5		36:20:20:20	7.5:4.17:4.17:4.17
C_8	0:1:1:0	2	0:48:48:0	0:10:10:0
C_9	1:1:1:0	3	32:32:32:0	6.67:6.67:6.67:0

allocation in the network. AMSs in each cell are only able to modulate PRUs in their assigned FP but not in any other FPs. The maximum number of PRUs in each FP is denoted by N and each PRU is denoted by \mathcal{P}_k where $k = \{1, 2, \dots, N\}$. For any DFPC used in the network, the number of utilized FPs is known as the frequency partition count (FPCT) and the number of PRUs allocated to each FP is known as the frequency partition size (FPS) [4].

AFFR mechanism in WiMAX indicates a maximum number of DFPCs to be used in the network. The maximum number of utilized DFPCs in the network is \mathbb{C} and each DFPC is denoted by C_c where $c = \{1, 2, \dots, \mathbb{C}\}$. The maximum number of utilized DFPCs is determined according to the utilized bandwidth and the employed fast fourier transform (FFT) in the network. The bandwidth and FP bandwidth are denoted by \mathcal{W} and \mathcal{W}_i respectively.

4 DFPC AND POWER ALLOCATION

This section aims at understanding the DFPC and the power allocation mechanism introduced in WiMAX. This interpretation is crucial in formulating the problem and identifying the optimal DFPC.

4.1 Down-Link Frequency Partition Configuration

WiMAX regulates a maximum of four FPs in the network. The utilized DFPC determines the FPCT in the network that ranges from one to four FPs. In case FPCT is greater than 1, each ABS in the network uses FP (\mathcal{F}_0) in the cell center. In case of reuse-2, each ABS uses only one of the two FPs (\mathcal{F}_1 , \mathcal{F}_2) in the cell edge. In case of reuse-3, each ABS uses only one of the three FPs (\mathcal{F}_1 , \mathcal{F}_2 , \mathcal{F}_3) in the cell edge. Fig. 2 shows a reuse-3 network configuration with four FPs where FP (\mathcal{F}_0) is used in the cell center and FPs (\mathcal{F}_1 , \mathcal{F}_2 , \mathcal{F}_3) are used in the cell edge.

Identifying the optimal DFPC is affected by the network topology, load conditions, and users distribution. Table 2 presents a detailed description of the DFPCs that can be used in a network with the 20 MHz bandwidth and FFT Size = 2048. Other tables are offered in [4] to networks with different bandwidth and FFT sizes. Each row in Table 2 specifies one of the DFPCs, for example a network that uses DFPC (C_4) has four FPs (FPCT = 4), \mathcal{F}_0 is the cells center FP and its size is three times the size of the cells edge FPs in the network (3:1:1:1). The number of PRUs (FPS) allocated to \mathcal{F}_0 to be distributed on the AMSs are 48 PRUs with a total bandwidth \mathcal{W}_0 of 10 MHz. Similarly (\mathcal{F}_1 , \mathcal{F}_2 , \mathcal{F}_3) are three

equal cell edge FPs, according to DFPC (C_4) each edge FP is allocated 16 PRUs to be distributed on its AMSs with a total bandwidth of 3.33 MHz for each FP ($\mathcal{W}_1:\mathcal{W}_2:\mathcal{W}_3$).

Four groups with the same FPCT are illustrated in Table 2;

- 1) Group 1 includes (C_1) with FPCT = 1.
- 2) Group 2 includes (C_8) with FPCT = 2.
- 3) Group 3 includes (C_2, C_9) with FPCT = 3.
- 4) Group 4 includes (C_3, C_4, C_5, C_6, C_7) with FPCT = 4.

For interference mitigation purposes, only one group is assumed to be used in the network at any time instance. However, the network can switch between different groups every DFPC update interval (T). Once the operating groups is chosen based on to the network topology, the optimal DFPC can be identified from within the chosen groups DFPCs. However in case of disconnected networks with multiple subsets controlled under the same HNCE, the HNCE can choose a different DFPC group for each subset. The optimal DFPC changes on semi-static basis in order to adapt with the variations in the network load conditions and users distribution in the network.

4.2 Power Allocation Mechanism

AMSs in cell center experience good channel conditions but need to control their power transmission levels to avoid ICI. However, AMSs in the cell edge suffer from bad channel conditions that require them to boost their transmission power levels. WiMAX adopts an AFFR power allocation mechanism that aims at both preventing ICI and improving NSE.

4.2.1 AFFR Power Allocation Mechanism

The power pattern presentation in Fig. 2 shows an example of the AFFR power allocation mechanism. Regular, boosted, and de-boosted transmission power levels are utilized in each cell. AFFR uses different power patterns for each group of neighbor cells; ABSs in cells (1), (2, 3, 4), and (5, 6, 7) use patterns (2), (3), and (1) respectively. ABS segment IDs are used for managing the power patterns utilization in the network by ensuring that neighbor ABSs use different power patterns [4].

Power patterns in the cell center shown in Fig. 2 has a regular power level range (P_0) for (\mathcal{F}_0) and power de-boosted levels range of (P_2, P_3) for ($\mathcal{F}_2, \mathcal{F}_3$). In the cell edge, however, the power patterns has power boosted level range (P_1) for (\mathcal{F}_1). Controlling the power de-boosted levels (P_2, P_3) helps avoid ICI generated from the cell center AMSs, while controlling the power boosted level (P_1) in the cell edge enhance the NSE.

4.2.2 Power Allocation for Frequency Partitions

The maximum transmission power level in each cell is defined by P_{max} . FP (\mathcal{F}_0) is reused in the center of each cell with a fixed maximum power level ($P_{0,max}$) FPs ($\mathcal{F}_1, \mathcal{F}_2, \mathcal{F}_3$) are reused with a maximum power boosted level ($P_{1,max}$) in the cell edges and a maximum power de-boosted levels ($P_{2,max}, P_{3,max}$) in the cell center. In general, the maximum power $P_{i,max}$ in each FP is calculated according to (1).

$$P_{i,max} = \begin{cases} P_{0,max} = \alpha P_{max} & \alpha < 1, \\ P_{1,max} = \beta P_{max} & \beta = 1, \\ P_{2,max}, P_{3,max} = \gamma P_{max} & \gamma \ll < < 1, \end{cases} \quad (1)$$

where α, β, γ are the power control factors used to determine the value of $P_{i,max}$ and $\alpha, \beta, \gamma = 0$ for non-existing FP in any DFPC [13].

4.3 Spectral Efficiency

In order for ABSs to determine the optimal local DFPC, at system entry each AMS in the cell is required by the ABS to calculate it's achievable NSE for all cell FPs. The AMSs compare the values of the NSE in all FPs and identify the FP with the maximum calculated NSE. AMSs inform the ABS by their preferred frequency partition (PFP) using the preferred frequency partition indicator (PFPI). The feedback from the AMSs support the ABS decisions to admit AMSs into different cell FPs.

4.3.1 SINR and Rate Calculations

The signal to interference plus noise ratio (SINR) threshold model proposed in [13] is adopted. SINR experienced when allocating PRU (\mathcal{P}_k) at cell (\mathcal{L}_b) FP (\mathcal{F}_i) to AMS (\mathcal{S}_j) is denoted by $SINR_{bijk}$. AMSs are classified in the cell regions according to their SINR threshold denoted by δ_b into cell center or cell edge AMSs. AMSs with $SINR_{bijk} \geq \delta_b$ are classified as cell center AMSs, and AMSs with $SINR_{bijk} < \delta_b$ are classified as cell edge AMSs. Adaptive modulation and coding (AMC) is assumed, AMSs adjust their transmission constellation according to the channel state conditions; in case of good channel conditions AMSs use a high order modulation while in case of poor channel condition a low modulation order is used. The AMC constellation (e.g. QAM) is selected in the ABS by the link adaptation procedure according to the SINR exhibited by each AMS and regularly reported to the ABS. The SINR is calculated according to (2)

$$SINR_{bijk} = \frac{P_{bijk} G_{bijk}}{\sum_{v \in I_l} P_{livk} G_{livk} + N_0 w}, \quad (2)$$

where P_{bijk} is the power consumed for allocating PRU (\mathcal{P}_k) to AMS (\mathcal{S}_j) in cell (\mathcal{L}_b) FP (\mathcal{F}_i), P_{livk} is the power consumed for allocating PRU (\mathcal{P}_k) to AMS (\mathcal{S}_v) in all interfering cells (\mathcal{L}_l) FP (\mathcal{F}_i), where $v \in I_l$ and I_l is the set of interfering AMSs to AMS (\mathcal{S}_j) that uses the same FP (\mathcal{F}_i) in all interfering cells (\mathcal{L}_l). N_0 is the thermal noise density and w is the sub-carriers separation. G_{bijk} is the channel gain experienced by AMS (\mathcal{S}_j) in cell (\mathcal{L}_b) FP (\mathcal{F}_i) on PRU (\mathcal{P}_k), G_{livk} is the channel gain experienced by AMS (\mathcal{S}_v) in cell (\mathcal{L}_l) FP (\mathcal{F}_i) on PRU (\mathcal{P}_k). The channel gain is calculated as shown in (3)

$$G_{bijk} = 10^{-\frac{\Gamma_{bijk}(d)}{10}} \omega_{bijk} \zeta_{bijk}, \quad (3)$$

where $\Gamma_{bijk}(d)$ is the path loss at distance d . ω_{bijk} and ζ_{bijk} are the shadowing and fading coefficient respectively [14].

According to the Shannon's theorem, the data rate r_{bijk} achieved by each AMS can be expressed as shown in (4)

$$r_{bijk} = w \log_2(1 + \lambda SINR_{bijk}), \quad (4)$$

where $\lambda = \frac{-1.5}{\ln(5 * BER)}$ and BER is the Bit Error Rate [5].

For each cell (\mathcal{L}_b) FP (\mathcal{F}_i) the achieved throughput denoted by \mathcal{R} is calculated as shown in (5)

$$\mathcal{R}_{bi} = \sum_{j=1}^S \sum_{k=1}^N w \log(1 + \lambda \text{SINR}_{bijk}). \quad (5)$$

The total throughput is the sum of the achievable throughput in cell (\mathcal{L}_b) FP (\mathcal{F}_i) by all AMSs according to the PRUs allocation results from solving the optimization problem by each ABS.

4.3.2 Normalized Spectral Efficiency

The NSE calculated as shown in (6) specifies how efficiently the limited frequency spectrum is utilized.

$$\text{NSE}_{ijk} = \frac{\text{ESE}_{ijk}}{RM_i}, \quad (6)$$

where ESE_{ijk} and RM_i are AMS (\mathcal{S}_j) expected spectral efficiency from allocating PRU (\mathcal{P}_k) in FP (\mathcal{F}_i) and the resource metric (RM) in FP (\mathcal{F}_i) respectively.

4.3.3 Expected Spectral Efficiency

The ESE is calculated according to (7)

$$\text{ESE}_{ijk} = \frac{r_{ijk}(1 - \text{PER})}{\mathcal{W}_i}, \quad (7)$$

where r_{ijk} and \mathcal{W}_i are the AMS expected data rate and FP bandwidth respectively. PER is the AMS estimated Packet Error Rate.¹ The expected value of the PER is denoted by packet error probability E_p . For a data packet length of n bits, E_p is calculated as shown in (8)

$$E_p = 1 - (1 - b_e)^n, \quad (8)$$

where b_e is the bit error probability, b_e is equal to the expected value of the BER.

4.4 Resource Metric Information

AMSs periodically check their achievable NSE for all cell FPs in order to update the ABS by their PFP. In order to obtain more distributed control, WiMAX employs a resource metric information that impacts the calculation of the NSE. Each ABS periodically sends the RM information in each super-frame to all AMSs in the cell. AMSs utilize the RM values to calculate the NSE. The RM values selected by each ABS changes the values of the AMSs achievable NSE and impacts their selection for the PFP.

The NSE calculated by each AMS depends on the RM values indicated by the ABS. RM_i for networks with reuse-3 and reuse-2 is calculated for different FPs \mathcal{F}_i according to (9) and (10) respectively [4].

$$RM_i = \begin{cases} 1 & i = 0, \\ 3 - RM_2 - RM_3 & i = 1, \\ 0 \leq RM_2 < 1 & i = 2, \\ 0 \leq RM_3 < 1 & i = 3, \end{cases} \quad (9)$$

1. PER presents the number of incorrectly received data packets divided by the total number of received packets. A packet is declared incorrect if at least one of the packet bits is erroneous.

$$RM_i = \begin{cases} 1 & i = 0, \\ 2 - RM_2 & i = 1, \\ 0 \leq RM_2 < 1 & i = 2, \end{cases} \quad (10)$$

where RM_2 and RM_3 are the values for the resource metric for FPs \mathcal{F}_2 and \mathcal{F}_3 respectively. RM_2 and RM_3 are assumed as a random values in the allowed range in (9) and (10). The ABS transmits the resource metric values as a quantized fractional number "y" between zero and one. Each AMS receives and decodes the quantized resource metric to determine the RM real value [4]. The identification of the optimum values of RM_2 and RM_3 is important in balancing the load between different FPs, however, its not considered in the scope of this paper.

The following brief example is used to clarify the effect of the RM values on the calculations of the NSE. In case of reuse-3 for the lower bound $RM_2 = 0$, the calculated NSE by the AMSs in \mathcal{F}_2 will tend to infinity which will be a reason for the these AMSs to choose \mathcal{F}_2 as their PFP. However in case of upper bound $RM_2 \simeq 1$, the calculated NSE by the AMSs in \mathcal{F}_2 will be approximately equal to the expected calculated ESE which will prevent the AMSs from joining \mathcal{F}_2 if the ESE is low or at least not competitive enough to other FPs. Similar to RM_2 , the values RM_3 have the same effect on the calculations of the NSE in \mathcal{F}_3 . The changes in RM_2 and RM_3 are significant to the calculations of RM_1 as shown in (9). RM_1 values increases and the expected NSE achieved in \mathcal{F}_1 decreases if RM_2 and RM_3 decreases and vice versa. This results in the variation of the AMSs decision to choose \mathcal{F}_1 as their PFP.

4.5 Utility Update Intervals

The maximum expected central utility is calculated every DFPC update interval denoted by T while the maximum expected distributed utility is calculated every optimization calculation interval denoted by t . There is a dependency between t and T values, the value of t shall be less than T and a suitable t interval should be selected to present the network dynamics. For example $T = 5t$ implies that the maximum central utility is calculated using five calculated samples of the maximum distributed utility during T interval.

The sampling rate is determined according to the value of the sampling factor denoted by $\tau = \frac{T}{t}$. The optimum value of τ is important, a larger sampling rate (e.g. 50 samples/sec, sample each super frame) increases the accuracy of the optimal solution, however, a small sampling rate (e.g. 5 samples/sec, sample each 10 super frames) decreases the load incurred on the ABSs from solving the optimization problem. Thus for a T interval of 1 hr with high sampling rate $\tau = 180,000$ sample is needed while for low sampling rate $\tau = 18,000$ sample. This trade-off between accuracy and computational load needs to be addressed before choosing the optimal sampling factor (τ).

In WiMAX, T ranges from 1 to 143,200 minutes (≈ 99.4 days) with a default of 1 hr [4]. T duration controls the dynamics of the DFPC utilized in the network. Moreover, t duration specifies the accuracy of the maximum central utility calculations. Suitable selection of τ increases the accuracy of the optimal solution, and decreases the load

incurred on ABSs due to the iterative calculation of the optimal distributed utility.

In the proposed scheme, the optimal distributed utility and the DFPC achieving it are calculated in the ABSs. Therefore a message must be communicated between each ABS and the HNCE. This message is responsible for updating the HNCE by the values of the distributed utility and their corresponding DFPC numbers. This will be an 18-20 bytes message send by each ABS to inform the HNCE with the needed information to calculate the maximum central utility and to identify the optimal DFPC. The communication between the ABSs and the HNCE incur an overhead which is proportional to the number of the ABSs in the network.

5 UTILITY AND PROBLEM FORMULATION

The two phase problem aims at identifying the the optimal DFPC to be implemented in the network. The distributed phase calculates the PRUs allocation matrix X_b and determines the optimal DFPC locally in each cell \mathcal{L}_b by using a newly proposed distributed utility function. The central phase calculates the DFPCs allocation matrix X_c and identifies the optimal DFPC globally in the network by using a central utility function. The objective of these scheme is to jointly maximize the NSE and minimize the power consumption in the network.

5.1 Utility Function Formulation

The proposed scheme uses two utility functions to identify the optimal DFPC. The distributed phase utility function denoted by U_b is calculated locally by each ABS and the central phase utility function denoted as U_c is calculated globally by a HNCE for the network.

5.1.1 Scheme Distributed Phase “Utility Function”

The objective of the proposed distributed utility is to increase the ROI of the MSPs' by jointly increasing the NSE and decreasing the consumed power. In order to achieve this objective, the utility is selected in a manner that minimize the calculation load incurred on the ABSs. As previously mentioned, the AMSs periodically check their achievable NSE and report it to the ABSs and also the calculations of the consumed power is a regular task performed by the AMSs. However, other forms of the utility can be adopted to achieve the same objective but with extra calculation cost. The utility achieved by each AMS is denoted by U_{ijk} . The AMS utility is calculated as shown in (11):

$$U_{ijk} = \frac{NSE_{ijk}}{P_{ijk}}, \quad (11)$$

where NSE_{ijk} and P_{ijk} are the NSE achieved and the power consumed respectively due to the allocation of PRU (\mathcal{P}_k) to AMS (\mathcal{S}_j) in FP (\mathcal{F}_i).

U_b is the sum of the utility achieved by all AMSs in each cell \mathcal{L}_b . U_b is calculated by each ABS according to (12):

$$U_b = \sum_{i=1}^M \sum_{j=1}^S \sum_{k=1}^N U_{ijk}. \quad (12)$$

The maximum distributed utility achieved by each ABS during t interval is denoted by $U_{b,max}$ and the maximization problem that calculate $U_{b,max}$ is addressed in Section 5.2.1.

5.1.2 Scheme Central Phase “Utility Function”

The central utility denoted by U_c is the sum of $U_{b,max}$ per C_c achieved by all ABSs in the network. The HNCE calculates U_c as shown in (13):

$$U_c = \sum_{b=1}^B U_{b,max}/B, \quad (13)$$

for each DFPC the central utility calculated by the HNCE each T interval using $U_{c,s}$ reported by the ABSs each t interval is denoted by $U_{c,T}$ and expressed as

$$U_{c,T} = \sum_{t=1}^T U_{c,t}. \quad (14)$$

The maximum central utility that determine the DFPC to be implemented in the network is denoted by $U_{c,max}$ and the maximization problem that calculate $U_{c,max}$ is addressed in Section 5.2.2.

5.2 RRM Model

The proposed RRM model is executed using a two phase (centralized and distributed) approach; The first phase solves a distributed problem each optimization calculation interval (t) implemented locally by each ABS. The objective of the scheme distributed phase is to calculate $U_{b,max}$. The second phase solves a centralized problem each DFPC update interval (T) implemented globally by a HNCE. The objective of the scheme central phase is to calculate $U_{c,max}$ and to identify the optimal DFPC to be utilized in the network.

5.2.1 Scheme Distributed Phase “Problem Formulation”

Each ABS calculates the AMSs expected achievable data rates $E[r_{ijk}]$ for all current group DFPCs. The AMSs expected SINR $E[SINR_{ijk}]$ values for all current group DFPCs are assumed to be the same as the current measured SINR values. In order to calculate the AMSs expected utility $E[U_{ijk}]$, each ABS calculates the AMSs expected $E[NSE_{ijk}]$ and the expected power consumption $E[P_{ijk}]$ for all current group DFPCs. After calculating the $E[U_{ijk}]$, the ABS solves the joint optimization problem and calculates the expected maximum distributed utility $E[U_{b,max}]$ for all the current group DFPCs. The ABS reports the maximum distributed utilities and their corresponding DFPCs to the HNCE.

The distributed phase joint optimization problem for each C_c is modeled to calculate $U_{b,max}$ as shown in (15) to (21).

$$\arg \max_{X_b} \sum_{i=1}^M \sum_{j=1}^S \sum_{k=1}^N U_{ijk} x_{ijk}, \quad (15)$$

$$s.t. \sum_{i=1}^M \sum_{j=1}^S \sum_{k=1}^N P_{ijk} x_{ijk} \leq P_{max}, \quad (16)$$

$$P_{ijk}x_{ijk} \leq P_{i,max}, \quad (17)$$

$$\sum_{k=1}^N r_{ijk} \geq r_{ijk,min}, \quad (18)$$

$$\forall (j = 1, 2, \dots, S), \quad (19)$$

$$\sum_{i=1}^M \sum_{j=1}^S \sum_{k=1}^N x_{ijk} = 1, \quad (20)$$

$$x_{ijk} = \{0, 1\}, \quad (21)$$

where U_{ijk} is the utility function achieved by AMS (S_j) using PRU (P_k) in FP (\mathcal{F}_i). The maximum ABS transmission power constraint in (16) states that the total power assigned to all AMSs are limited by ABS maximum power P_{max} . The power constraint in (16) ensures that AMSs in each FP limit their maximum transmission power to $P_{i,max}$. The constraint in (18) shows that the achievable rate requirement for each AMS should guarantee the minimum rate requirement $r_{ijk,min}$. This minimum rate is required to satisfy the QoS in the system. The binary variables x_{ijk} are the assignment indicators of the assignment matrix X_{br} and $x_{ijk} = 1$ if PRU (P_k) at FP (\mathcal{F}_i) is assigned to AMS (S_j) and $x_{ijk} = 0$ otherwise. The constraint on x_{ijk} in (21) and (20) ensures that each PRU is assigned to one and only one AMS. This problem's affine objective and constraint functions together with the integrality constraint construct a convex ILP optimization problem[15].

5.2.2 Scheme Central Phase "Problem Formulation"

The optimal DFPC is identified by solving the U_c maximization problem. The problem modeled in (15) to (20) calculates $U_{b,max}$ for each C_c in each cell. The U_c maximization problem aims to calculate $U_{c,max}$ and determine optimal DFPC from all possible DFPCs. Each ABS sends the values of the optimal distributed utilities each t interval with their corresponding C_c s to the HNCE. The HNCE utilizes this information to calculate the $U_{c,T}$ achieved during the T interval by solving the problem modeled in (22):

$$\arg \max_{X_c} U_{c,T}x_{c,T}, \quad (22)$$

$$x_{c,T} = \{0, 1\}, \quad (23)$$

where the binary variables $x_{c,T}$ are the assignment indicators for the assignment vector $X_{c,T}$, c is the configuration number and T is the allocation time. $x_{c,T} = 1$, if C_c is a possible DFPC and $x_c = 0$, otherwise. $U_{c,T}$ is the sum of the U_c calculated every interval t during T interval for each C_c as shown in (14). Every T interval, the HNCE compares the $U_{c,T}$ s for all DFPCs by solving the trivial optimization problem in (22) to select the DFPC with $U_{c,max}$. The DFPC with $U_{c,max}$ is the selected optimal DFPC to be implemented in the network.

6 PROBLEM SOLUTION

6.1 Optimal Solution

6.1.1 Scheme Distributed Phase

The distributed phase problem to be solved by each ABS is a binary ILP optimization problem. This problem is classified as NP-hard problem with high computational complexity when optimally solved. It's solved by determining $U_{b,max}$ per DFPC in each ABS.

6.1.2 Scheme Central Phase

After determining $U_{b,max}$ per DFPC in each ABS, $U_{c,T}$ is incremented in the HNCE by $U_{b,max}$ every t interval to calculate $U_{c,T}$ achieved by each DFPC. The $U_{c,T}$ s for all DFPCs are then compared to determine $U_{c,max}$ and identify its corresponding DFPC to be utilized in the network.

6.2 Suboptimal Solution

6.2.1 Scheme Distributed Phase "Greedy Heuristic Algorithm"

The optimal solution of the U_b maximization problem (ILP problem) is limited by its high computational complexity. This limitation appears significantly in case of short T intervals (e.g $T = 1$ min) when the problem optimal solution is required within T time frame. A suboptimal solution using a greedy algorithm is used to overcome this limitation. Algorithm 1 presents the greedy heuristic implemented by each ABS in the network.

Algorithm 1. Greedy Heuristic

for $t < T$ do

Inputs: (C);(M);(S);(N);($P_{b,max}$);($P_{i,max}$);
 ($[U_{ijk}]$);($[P_{ijk}]$);(t);(T)

Initialize: ($[U_{b,max}] = 0$); ($[P_b] = 0$);
 ($[U_c] = 0$);($[U_{c,T}] = 0$);($[U_{c,max}] = 0$)

Sort: ($[U_{ijk}]$) /* Sort ($[U_{ijk}]$) in descending order */

Sort: ($[P_{ijk}]$) /* Sort ($[P_{ijk}]$) in corospondance to
 ($[U_{ijk}]$) */

 for $c \leq C$ do

 for $i \leq M$ do

 for $j \leq S$ do

 for $k \leq N$ do

 while $P_b \leq P_{b,max}$ do

 if $P_{ijk} \leq P_{i,max}$ then

State: $U_{b,max} = U_{b,max} + U_{ijk}$

State: $P_b = P_b + P_{ijk}$

 end

 end

 end

 end

 end

 end

Return: ($U_{b,max}$) & (C_c) /* (C_c) Corosponding to ($[U_{b,max}]$) */

State: $t = t + 1$

end

Algorithm 1 starts every time interval t by requesting inputs and initializing variables. For all expected DFPCs the U_{ijk} matrices and their corresponding P_{ijk} matrices are arranged in a decreasing order. For each DFPC, $U_{b,max}$ is

calculated for all cell FPs by iterating through the U_{ijk} sorted matrices, incrementing U_{ijk} and P_{ijk} . Each iteration, the power constraints per ABS ($P_{b,max}$) and per FP ($P_{i,max}$) are checked for satisfaction. Finally, the algorithm returns the $U_{b,max}$ and its corresponding C_c for all DFPCs.

6.2.2 Scheme Central Phase “Utility Maximization Algorithm”

The optimal solution of the U_c maximization problem is of low complexity; however, for practical implementation purposes we recommend Algorithm 2 to be used by the HNCE to calculate $U_{c,max}$.

Algorithm 2. Central Utility Maximization

Inputs: $(B); ([U_{b,max}]); (C); (t); (T)$
Initialize: $([U_c] = 0); ([U_{c,T}] = 0); ([U_{c,max}] = 0)$
for $t < T$ **do**
 for $c \leq C$ **do**
 for $b \leq B$ **do**
 State: $U_c = \sum_{b=1}^B (U_{b,max}) / B$
 end
 State: $U_{c,T} = U_{c,T} + U_c$
 end
 State: $t = t + t$
 end
Return: $[U_{c,T}]$ & $[C_c] / *(C_c)$ Corrospounding to $([U_{c,T}])$ * /
if $t = T$ **then**
 Compare: $[U_{c,T}]$
 $\forall (C_c : c = 1, 2, \dots, C)$
 State: $U_{c,max} = \max(U_{c,T})$
end
Return: $(U_{c,max})$ & $(C_c) / *(C_c)$ Corrospounding to $([U_{c,max}])$ * /

Algorithm 2 starts by requesting inputs and initializing variables. Every time interval T , U_c is used to calculate $U_{c,T}$ for all DFPCs in the network. $U_{c,T}$ s for all DFPCs are compared and finally, the algorithm returns $U_{c,max}$ and the optimal DFPC to be implemented in the network.

6.3 Complexity Analysis for Suboptimal Solution

Discussing the efficiency of Algorithm 1 (greedy heuristic) is essential to prove its ability for practical implementation. The computational complexity of the greedy heuristic is analyzed by analyzing the worst case running time of the algorithm.

Initially, in each ABS, the algorithm sorts and labels all U_{ijk} for all DFPCs in a descending order. This step takes time $O(CMSN \log MSN)$ to sort the utility arrays and an additional time $O(CMSN)$ to label the sorted arrays. $U_{b,max}$ is calculated by iterating through the AMSs sorted utility array incrementing U_{ijk} while checking for the violation of power constraints. This step incurs a maximum time $O(CMSN)$ to get accomplished.

The worst case running time is calculated by summing up the times required to run the algorithm. Algorithm 1 needs a total $O(CMSN \log MSN)$ to calculate $U_{b,max}$ for all DFPCs. The computational complexity analysis for the worst case running time shows that Algorithm 1 is a polynomial-time algorithm.

Algorithm 2 incur a polynomial worst case running time $O(CB\tau)$ to calculate $U_{c,max}$ that identifies the optimal DFPC

TABLE 3
System Parameters

Parameter	Value
Number of Cells (B)	7
Number of FPs (M)	4
Number of AMSs (S)	60
Number of PRUs (N)	96
Number of DFPCs (c)	$5(C_2 - C_6)$
BER	10^{-6}
ABS Maximum Power (P_{max}) [w]	10
SINR Threshold (δ_b) [db]	18.5
DFPC Update Interval (T) [hr]	1
Optimization Calculation Interval (t) [Sec]	20
Bandwidth (W_i) [MHZ] $\{(F_0)/(F_1, F_2, F_3)\}$	(20){(10)/(3.33)}

to be used in the network. Finally, the analysis of the worst case running time for calculating $U_{b,max}$ in algorithm 1 and $U_{c,max}$ in algorithm 2 shows that both algorithms are polynomial-time suitable for practical implementation.

The computation time for running the greedy heuristic is measured in addition to the computational complexity to show the time frame needed to execute the algorithm. The computational time is calculated on a Linux machine (x86_64) with *Intel Xeon* CPU (X5550 @ 2.67 GHz) and 94.5 GB RAM. A number of 60 AMSs are allocated 96 PRUs in both FPs of a single ABS using configuration C_3 to show the allocation time needed by the greedy heuristic to perform the allocation process. The computational time for the allocation is calculated as (389 ms) under the aforementioned conditions.

7 SIMULATION AND RESULTS

7.1 Optimal Solution

This section presents the simulation and results of the proposed optimal solution. We run the simulation to calculate $U_{c,max}$ and identify the optimal DFPC. Cplex is used to solve the problem and to calculate the X_{ijk} that achieves $U_{b,max}$. After determining $U_{b,max}$ per DFPC in each ABS, a Java program is developed to increment the values of $U_{b,max}$ generated by Cplex every t interval to calculate $U_{c,T}$ achieved by each DFPC.

Three different schemes aiming at maximizing different objectives are adopted in the simulation. First scheme denoted as S_1 represents our scheme that maximize the central utility (U_c), the second scheme denoted as S_2 only maximizes the normalized spectral efficiency, and the third scheme denoted as S_3 maximizes the achieved throughput (\mathcal{R}). Different DFPCs are used in the simulation, the results for a network that utilizes DFPCs from group 4 (C_2 to C_6) are presented and the parameters used in the simulation are described in Table 3.

A performance comparison between our proposed scheme S_1 and optimization schemes S_2 and S_3 is presented. The performance evaluation of S_1 against S_2 meant to clarify the difference between them in terms of NSE and power consumption due to the consideration of the power consumption in the formulation of S_1 . In addition, the performance evaluation of S_3 is intended to show a comparison between our proposed scheme S_1 and rate adaptive resource allocation schemes such as those presented in [5], [6].

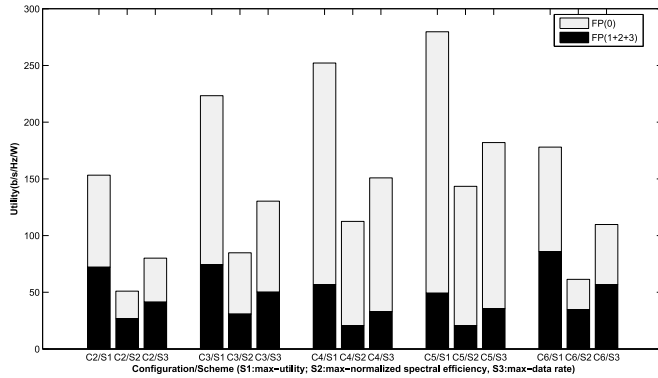


Fig. 3. Comparison between U_c achieved by S_1 , S_2 , and S_3 in cells center FP (\mathcal{F}_0) and cells edge FPs ($\mathcal{F}_1, \mathcal{F}_2, \mathcal{F}_3$).

The results in Fig. 3 show that $U_{c,max}$ in the network and in cells center FP (\mathcal{F}_0) are achieved by C_5/S_1 . $U_{c,max}$ in cells edge FPs ($\mathcal{F}_1, \mathcal{F}_2, \mathcal{F}_3$) is achieved by C_6/S_1 . The previous finding indicates that, in case of high load condition in cells edge, using C_6/S_1 instead of C_5/S_1 can boost $U_{c,max}$ by using a DFPC that assigns more resources to the cells edge users. This result shows the effect of the network load conditions and users distribution on the dynamics of the chosen DFPC that achieves $U_{c,max}$.

The results in Fig. 4 show a comparison between the NSE for group 4 DFPCs. The maximum network NSE is achieved by C_5/S_2 . However, the achieved NSE by C_5/S_1 the DFPC with $U_{c,max}$ is lower than C_5/S_2 due to the influence of minimizing the power consumption considered by C_5/S_1 on maximizing the NSE. S_2 maximizes the NSE without considering the amount of power consumed by selecting users with maximum NSE without considering their power consumption requirements. The results show 1 (b/s/Hz) difference between NSE achieved by C_5/S_1 and C_5/S_2 .

Fig. 4 shows that C_5/S_2 achieves the maximum NSE in cells center FP (\mathcal{F}_0) which is the same DFPC that achieve $U_{c,max}$. Moreover, the maximum NSE in the cell edge FPs ($\mathcal{F}_1, \mathcal{F}_2, \mathcal{F}_3$) is achieved by C_2/S_2 not C_3/S_2 the DFPC with $U_{c,max}$ in the cells edge. This indicates that the consideration of minimizing the power consumption in the allocation process influences the DFPC identification decision.

The results in Fig. 5 shows that C_4/S_1 is the DFPC that consumes the minimum consumed power in both the network and in cells edge FPs ($\mathcal{F}_1, \mathcal{F}_2, \mathcal{F}_3$). Moreover, C_2/S_1 consumes the minimum consumed power in cells center

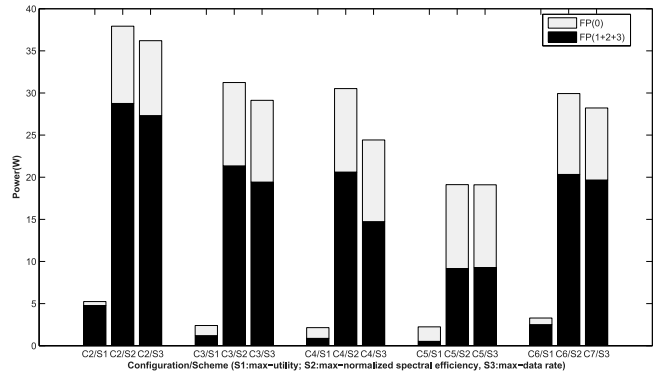


Fig. 5. S_1 , S_2 , and S_3 minimum power consumption comparison in cells center FP (\mathcal{F}_0) and cells edge FPs ($\mathcal{F}_1, \mathcal{F}_2, \mathcal{F}_3$).

FP (\mathcal{F}_0). Fig. 5 shows that C_5/S_1 the DFPC with $U_{c,max}$ consumes higher amount of power than C_4/S_1 , yet C_5/S_1 shows significant difference in the minimum amount of power consumed compared to C_5/S_2 the DFPC with maximum NSE. The large amount of power consumed by C_5/S_2 is due to either high data rates achieved by cell center users or poor channel conditions exhibited by users in the cell edge.

The results in Fig. 6 show a comparison between the maximum achievable \mathcal{R} for group 4 DFPCs. C_5/S_3 achieves maximum \mathcal{R} in both the network and cells center FP (\mathcal{F}_0). Moreover, C_2/S_3 achieves the maximum \mathcal{R} in the cells edge FPs ($\mathcal{F}_1, \mathcal{F}_2, \mathcal{F}_3$).

The achievable \mathcal{R} of C_5/S_1 the DFPC with $U_{c,max}$ is less than C_5/S_3 due to the consideration of the power consumption that enforces S_1 to choose users with both maximum \mathcal{R} and minimum amount of power consumed. The reason for the increase in $U_{c,T}$ achieved by C_5/S_1 over other S_1 DFPCs (C_2, C_3, C_4, C_6) is due to the users good channel conditions in the cells center which cause an increase in their achievable \mathcal{R} as shown in Fig. 6.

The results show that C_5/S_1 achieves $U_{c,max}$, C_5/S_2 achieves the maximum NSE, and C_5/S_3 achieves the maximum \mathcal{R} . These results indicate that although C_5 is the optimal DFPC to be used in the network but each allocation scheme utilizes C_5 generates a different ROI from the network.

Results in Fig. 7 are presented to show the effect of the proposed scheme S_1 on the system performance metrics (power and NSE). Results of the joint optimization using S_1

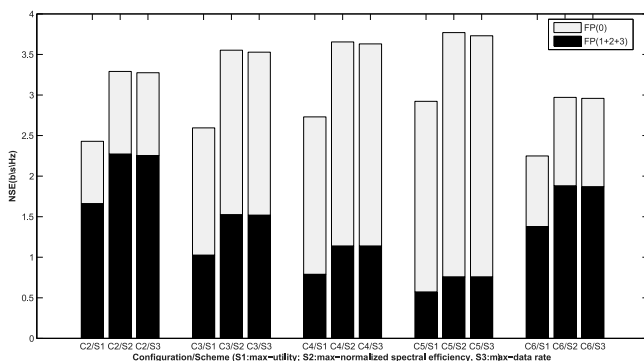


Fig. 4. Comparison between S_1 , S_2 , and S_3 maximum NSE in cells center FP (\mathcal{F}_0) and cells edge FPs ($\mathcal{F}_1, \mathcal{F}_2, \mathcal{F}_3$).

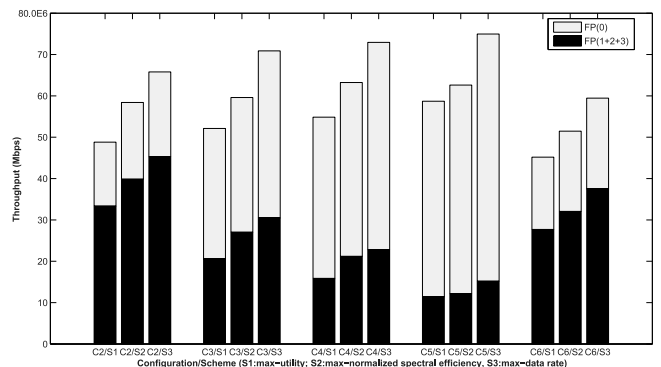


Fig. 6. Comparison between S_1 , S_2 , and S_3 maximum \mathcal{R} in cells center FP (\mathcal{F}_0) and cells edge FPs ($\mathcal{F}_1, \mathcal{F}_2, \mathcal{F}_3$).

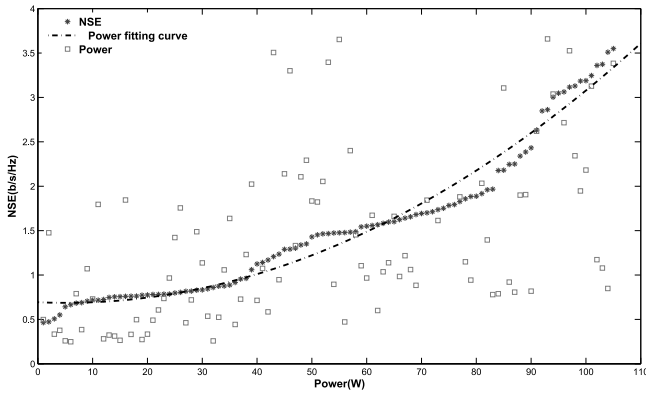


Fig. 7. Trade-off between the achieved NSE and consumed power using scheme S_1 .

shows a trade-off between the power consumption and the spectral efficiency. This trade-off appears in the form of an increase in the amount of power consumed with the increase in the achieved NSE.

7.2 Suboptimal Solution

A simulation is conducted to evaluate the efficiency of the suboptimal solution. Fig. 8 shows a comparison between the maximum U_c for S_1 and the greedy heuristic denoted by S_4 . The results show that the heuristic succeeded to identify the same DFPC (C_5) as the optimal DFPC. The results also show an approximate gap of 4 percent between S_1 and S_4 .

8 CONCLUSION

In this study, a RRM model that utilizes adaptive fractional frequency reuse mechanism in WiMAX is proposed to identify the optimal DFPC to be implemented in the network. The objective of the model is to improve the mobile service providers MSPs' return on investment by maximizing the NSE and minimizing the total power consumption in the network.

To solve the problem, we adopted a utility based optimization technique in which we proposed a central and distributed utility functions calculated by a higher network control entity and the ABS respectively. A joint optimization problem is formulated to calculate the distributed utility in each ABS and a utility maximization problem is formulated to calculate the maximum central utility in the network. The problem solution succeeded to calculate the maximum central utility and to identify the optimal DFPC to be utilized. The optimal solution though shows a high computational complexity. Thus, for practical implementation purposes a suboptimal heuristic called the greedy heuristic is additionally proposed to solve the problem.

A simulation for the proposed model shows accepted results and a comparison between the optimal and the suboptimal solutions is conducted to evaluate the suboptimal solution efficiency and investigate the gap with the optimal solution. Finally, this study proposes a RRM model that succeeded to maximize the NSE and to minimize the power consumed and we recommend our model for implementation by MSPs.

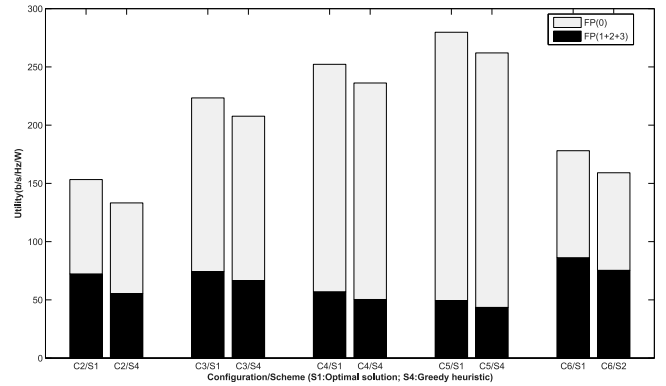


Fig. 8. S_1 versus S_4 : U_c maximization comparison in cells center FP (\mathcal{F}_0) and cells edge FPs ($\mathcal{F}_1, \mathcal{F}_2, \mathcal{F}_3$).

REFERENCES

- [1] IEEE 802.16m, *IEEE Standard for Local and metropolitan area networks Part 16: Air Interface for Fixed and Mobile Broadband Wireless Access Systems*, May 2009.
- [2] 3GPP, TR 25.814, *Physical Layer Aspects for Evolved UTRA*, 2009.
- [3] B. Harpham. (2010, Oct.). IEEE 802.16m approved as IMT-Advanced Technology. WiMAX Forum [Online]. Available: <http://wimaxforum.org/news/2650>
- [4] IEEE, *IEEE Standard for Local and metropolitan area networks Part 16: Air Interface for Broadband Wireless Access Systems Amendment 3: Advanced Air Interface*, 2011.
- [5] S. Ali and V. Leung, "Dynamic frequency allocation in fractional frequency reused OFDMA networks," *IEEE Trans. Wireless Commun.*, vol. 8, no. 8, pp. 4286–4295, Aug. 2009.
- [6] J. Kim and W. S. Jeon, "Two practical resource allocation techniques for fractional frequency reuse in IEEE 802.16m networks," in *Proc. 7th Int. Wireless Commun. Mobile Comput. Conf.*, Jul. 2011, pp. 261–265.
- [7] Z. Mohades, V. T. Vakili, S. M. Razavizadeh, and D. Abbasi-Moghadam, "Dynamic fractional frequency reuse (DFFR) with AMC and random access in WiMAX system," *Wireless Personal Commun.*, vol. 68, no. 4, pp. 1871–1881, Feb. 2013.
- [8] R. Chang, Z. Tao, J. Zhang, and C. Kuo, "A graph approach to dynamic fractional frequency reuse (FFR) in multi-cell OFDMA networks," in *Proc. IEEE Int. Conf. Commun.*, 2009, pp. 1–6.
- [9] R. Y. Chang, Z. Tao, J. Zhang, and C.-C. J. Kuo, "Dynamic fractional frequency reuse (D-FFR) for multicell OFDMA networks using a graph framework," *Wireless Commun. Mobile Comput.*, vol. 13, no. 1, pp. 12–27, 2011.
- [10] K. T. Kim, and S. K. Oh, "A universal frequency reuse system in a mobile cellular environment," in *Proc. IEEE 65th Veh. Technol. Conf.*, Apr. 2007, pp. 2855–2859.
- [11] N. Himayat, S. Talwar, A. Rao, and R. Soni, "Interference management for 4g cellular standards [wimax/lte update]," *IEEE Commun. Mag.*, vol. 48, no. 8, pp. 86–92, Aug. 2010.
- [12] G. Miao, N. Himayat, G. Li, A. Koc, and S. Talwar, "Interference-Aware Energy-Efficient Power Optimization," in *Proc. IEEE Int. Conf. Commun.*, Jun. 2009, pp. 1–5.
- [13] T. Novlan, R. Ganti, A. Ghosh, and J. Andrews, "Analytical evaluation of fractional frequency reuse for OFDMA cellular networks," *IEEE Trans. Wireless Commun.*, vol. 10, no. 12, pp. 1–12, Dec. 2011.
- [14] H. Lei, L. Zhang, X. Zhang, and D. Yang, "A novel multi-cell OFDMA system structure using fractional frequency reuse," in *Proc. IEEE 18th Int. Symp. Personal, Indoor Mobile Radio Commun.*, Sep. 2007, pp. 1–5.
- [15] S. Boyd and L. Vandenberghe, *Convex Optimization*. New York, NY, USA: Cambridge Univ. Press, 2004.



Tamer Omar received the BS degree in electrical engineering from Ain Shams University, Cairo, Egypt, and the Master's degree from the Arab Academy for Science and Technology, Alexandria, Egypt. He is currently working toward the PhD degree in the Department of Electrical Engineering, Iowa State University, Ames, IA. His research interests include wireless networks architecture, resources allocation in wireless network, and database management systems. He has more than nine years industrial experience in

different positions including being a programmer at the Iowa Department of Transportation and a system engineer at the Egyptian Petrochemical Holding Company.



Morris Chang received the MS and PhD degrees in computer engineering from North Carolina State University, Raleigh, NC. He joined Iowa State University, Ames, IA, in August, 2001. He was on the faculty of the Department of Electrical Engineering at Rochester Institute of Technology, Rochester, NY, from 1993 to 1995 and the Department of Computer Science at the Illinois Institute of Technology, Chicago, IL, from 1995 to 2001. He received the IIT University Excellence in Teaching Award in 1999. His

research interests include cyber security, wireless networks, energy-aware computing, and object-oriented systems. His research projects have been supported by US National Science Foundation (NSF), US Defense Advanced Research Projects Agency (DARPA), and Altera. Currently, he is a handling editor of the *Journal of Microprocessors and Microsystems*, and the Associate Editor-in-Chief of *IEEE IT Professional*. He is a senior member of the IEEE.

▷ **For more information on this or any other computing topic, please visit our Digital Library at www.computer.org/publications/dlib.**